A New Stereochemical Model from NMR for Benzoylated Cyclodextrins, Promising New Chiral Solvating Agents for the Chiral Analysis of 3,5-Dinitrophenyl Derivatives

Gloria Uccello-Barretta, Angela Cuzzola, Federica Balzano, Rita Menicagli, Anna Iuliano, and Piero Salvadori*

Centro di Studio del CNR per le Macromolecole Stereordinate ed Otticamente Attive, Dipartimento di Chimica e Chimica Industriale, via Risorgimento 35, 56126 Pisa-Italy

Received August 12, 1996[⊗]

Hexakis(2,3-di-*O*-benzoyl)-α-cyclodextrin and hexakis(2,3,6-tri-*O*-benzoyl)-α-cyclodextrin have been employed as chiral solvating agents (CSAs) for the NMR determination of the enantiomeric composition of derivatives of chiral amines, amino alcohols, alcohols, carboxyl acids, and amino acids bearing a 3,5-dinitrophenyl moiety. The conformational features of the two cyclodextrins have been carefully analyzed by NMR spectroscopy, and the origin of the symmetry change ($C_6 \rightarrow C_3$), detected by NMR for hexakis(2,3-di-*O*-benzoyl)-α-cyclodextrin in $CDCl_3$, has been clarified.

Introduction

Cyclodextrins[1a] are cyclic oligosaccharides having an apolar cavity where apolar moieties can be accommodated solely by means of hydrophobic interactions. Owing to their chirality, the interaction with chiral substrates can originate enantiodiscrimination phenomena. For this reason such chiral auxiliaries have received a great deal of attention for a long time both in asymmetric synthesis[1] and in the preparative or analytical separation of chiral compounds by chromatography.[2] In addition, cyclodextrins have found a very interesting application as chiral solvating agents (CSAs) for the determination of the enantiomeric purity by nuclear magnetic resonance (NMR).[3]

Recently we have reported that the commercially available permethylated *β*-cyclodextrin is a very efficient CSA for the NMR determination of the enantiomeric composition and absolute configuration of chiral trisubstituted allenes[4] and enantiomeric composition of aromatic hydrocarbons.[5]

These results prompted us to probe the efficiency as CSAs of other derivatized cyclodextrins; among them, we focused our attention on the hexakis(2,3-di-*O*-benzoyl)-α-cyclodextrin (**1**) and the hexakis(2,3,6-tri-*O*-benzoyl)-α-cyclodextrin (**2**) (Chart 1), for which previous investigations by NMR, carried out by Lehn[6] and Stoddart,[7] had evidenced the remarkable effect of the degree of benzoylation or solvent nature on their conformational features.

Chart 1

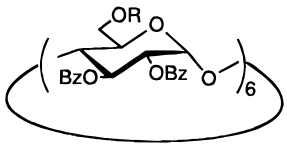

1 R=H
2 R=Bz

Bz = −C(=O)−Ph

In particular a conformationally flexible structure of **1**, in $CDCl_3$, having a three-fold symmetry axis was evidenced; in such a structure adjacent glucose residues twist each other around their glycosidic linkages. In this way three units point their benzoyl groups toward the inside of the cavity and their primary hydroxyl groups to the outside, whereas, for the other three units, the C_6 hydroxyl groups are directed toward the center of the cavity, thus creating a network of strong intramolecular hydrogen bonds (Figure 1). IR data were presented to support this hypothesis.[6,7]

In the present paper the use of **1** and **2** as CSAs for the NMR determination of the enantiomeric composition of 1-phenyl-1-(3′,5′-dinitrobenzamido)ethane (**3**), 1-cyano-1-(3′,5′-dinitrobenzamido)-2-methylpropane (**4**), *N*-(3,5-dinitrobenzoyl) derivatives of 2-amino-1-phenyl-1-propanol (**5a**), 2-amino-1-phenylethanol (**5b**), alanine methyl ester (**6**),[8] *t*-2-ethoxy-*r*-1-(hydroxymethyl)-1-methylcyclobutane (**7**),[9] and 3′,5′-dinitrophenyl-2-(*p*-isobutylphenyl)propionamide (**8**) (Chart 2) has been reported, and their enantiodiscriminating capability has been discussed. With the aim to obtain information on the interaction mechanisms involved in the chiral discrimination process, the conformational and dynamic features of **1** and **2** have been reexamined by an accurate NMR investigation in $CDCl_3$ or DMSO solution involving 2D ROESY (Rotating-frame Overhauser Enhancement SpectroscopY)[10] and ^{13}C longitudinal relaxation time measurements (T_1).[11] In addition, some attempts to detect

[⊗] Abstract published in *Advance ACS Abstracts,* January 1, 1997.

(1) (a) Szejtli, J. *Cyclodextrin Technology*; Kluwer: Boston, 1988. (b) Wenz, G. *Angew. Chem., Int. Ed. Engl.* **1994**, *33*, 803. (c) Bonchio, M.; Carofiglio, T.; Di Furia, F.; Fornasier, R. *J. Org. Chem.* **1995**, *60*, 5986. (d) Hattori, K.; Takahashi, K.; Sakai, N. *Bull. Chem. Soc. Jpn.* **1992**, *65*, 2690.

(2) (a) Francotte, E. *J. Chromatogr. A* **1994**, *666*, 565. (b) Li, S.; Purdy, W. C. *Chem. Rev.* **1992**, *92*, 1457. (c) Schurig, V.; Nowotny, H. P. *Angew. Chem., Int. Ed. Engl.* **1990**, *29*, 939. (d) Taylor, D. R.; Maher, K. *J. Chromatogr. Sci.* **1992**, *30*, 67. (e) Rogan, M. M.; Altria, K. D.; Goodall, D. M. *Chirality* **1994**, *6*, 25.

(3) (a) Greatbanks, D.; Pickford, R. *Magn. Reson. Chem.* **1987**, *25*, 208. (b) Casy, A. F.; Mercer, A. D. *Magn. Reson. Chem.* **1988**, *26*, 765.

(4) (a) Uccello-Barretta, G.; Balzano, F.; Caporusso, A. M.; Salvadori, P. *J. Org. Chem.* **1994**, *59*, 836. (b) Uccello-Barretta, G.; Balzano, F.; Caporusso, A. M.; Iodice, A.; Salvadori, P. *J. Org. Chem.* **1995**, *60*, 2227.

(5) Uccello-Barretta, G.; Balzano, F.; Menicagli, R.; Salvadori, P. *J. Org. Chem.* **1996**, *61*, 363.

(6) Boger, J.; Corcoran, R. J.; Lehn, J. M. *Helv. Chim. Acta* **1978**, *61*, 2190.

(7) Ellwood, P.; Spencer, C. M.; Spencer, N.; Stoddart, J. F.; Zarzycki, R. *J. Inclus. Phenom. Molec. Recogn. Chem.* **1992**, *12*, 121.

(8) Salvadori, P.; Pini, D.; Rosini, C.; Uccello-Barretta, G.; Bertucci, C. *J. Chromatogr.* **1988**, *450*, 163.

(9) Menicagli, R.; Malanga, C.; Lardicci, L. *J. Org. Chem.* **1982**, *47*, 2288.

S0022-3263(96)01562-9 CCC: $14.00

Scheme 1

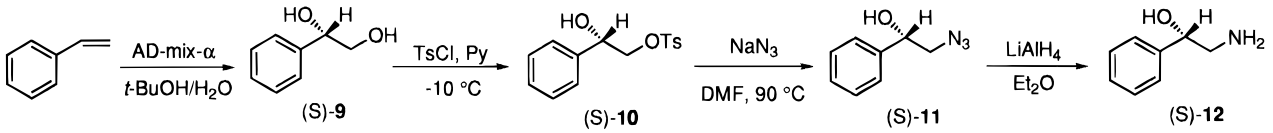

AD-mix-α = mixture of $(DHQ)_2PHAL$, $K_2OsO_2(OH)_4$, K_2CO_3, $K_2Fe(CN)_6$

$(DHQ)_2PHAL$ = hydroquinine 1,4-phthalazinediyl diether

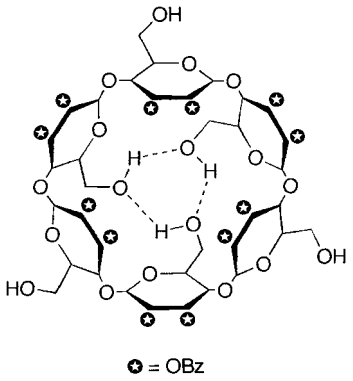

= OBz

Figure 1. Proposed[7] schematic representation of the structure of **1** in $CDCl_3$.

Chart 2

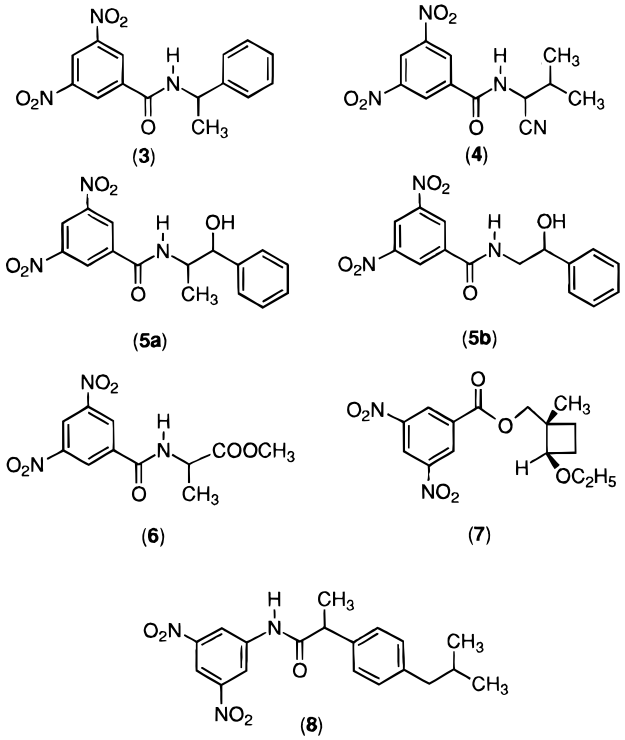

intermolecular dipolar interactions between each cyclodextrin and the chiral substrates have been made.

Results and Discussion

Synthesis of the Cyclodextrins 1, 2 and Chiral Substrates 3−5 and 8. The cyclodextrin derivatives **1** and **2** have been prepared according to the procedure reported by J. M. Lehn et al.[6]

The 3,5-dinitrobenzoyl derivatives **3** and **4** were prepared by reacting the corresponding available amines with 3,5-dinitrobenzoyl chloride in the presence of pyridine. Racemic **5a** as well as (*R*)- and (*S*)-**5b** and **8** were prepared by using EEDQ as condensing agent.[12]

As far as the two enantiomers of **5b** are concerned, they were prepared from the corresponding optically pure amino alcohols **12**, obtained by employing an efficient and practical route, which avoids the racemate optical resolution (Scheme 1).[13] The asymmetric catalytic dihydroxylation of styrene, according to the Sharpless method,[14] afforded (*R*)- or (*S*)-diol **9** in quantitative yield and 97% ee, when a quinidine or quinine derivative was used in the reaction, respectively.

Treatment of **9** with 1 equiv of tosyl chloride in pyridine at −10 °C[15] gave only the 1-hydroxy-2-tosyloxy derivative **10**. Reaction of **10** with sodium azide in dimethylformamide afforded the hydroxy azide **11**, which was successively reduced with $LiAlH_4$ to give the pure amino alcohol **12**.

Chiral Discriminations by 1 and 2. In order to probe the efficiency of **1** and **2** as chiral solvating agents for the NMR determination of the enantiomeric composition, the ^1H NMR spectra in $CDCl_3$ of the pure compounds **3**−**8** were compared with those of their corresponding equimolar mixtures with the cyclodextrin **1** or **2**.

In Figure 2 are reported the results obtained for **3** in the presence of the cyclodextrin **1** (Figure 2b) and of cyclodextrin **2** (Figure 2c). Both cyclodextrins produce doubling of the proton absorptions of **3**, to indicate that the originally enantiotopic protons became diastereotopic in the presence of the chiral auxiliary. Indeed, the 3,5-dinitrobenzoyl protons of **3** (Figure 2a), which produce two sharp signals at 9.15 ppm (triplet) and 8.94 ppm (doublet) in the free compound, exhibit in the presence of **1** (Figure 2b) two triplets at 9.08 ppm and 9.05 ppm and two partially superimposed doublets at 8.90 ppm and 8.89 ppm. As far as the methyl absorptions are concerned, producing the doublet centered at 1.68 ppm in the free compound, two superimposed doublets at 1.63 and 1.61 ppm (Figure 2b) are observed in the presence of the chiral auxiliary **1**. A minor but appreciable doubling of the aromatic protons signals is also observed in the presence of the cyclodextrin **2** (Figure 2c).

Compound **4** (Figure 3a) shows comparable doubling of the diastereotopic methyl absorptions of the isopropyl group in the presence of both **1** and **2** (Figures 3b, 3c).

In the case of **5a** (Figure 4), each CSA induces nonequivalence in the methyl absorptions, whereas only **1**

(10) Neuhaus, D.; Williamson, M. *The Nuclear Overhauser Effect*; VCH Publishers, Inc.: New York, 1989.

(11) Wehrli, F. W.; Wirthlin, T. *Interpretation of Carbon-13 NMR Spectra*; Heyden & Son Ltd.: London, 1976.

(12) Belleau, B.; Malek, G. *J. Am. Chem. Soc.* **1968**, *90*, 1651.

(13) Green, A. L.; Fielden, R.; Bartlett, D. C.; Cozens, M. J.; Eden, R. J.; Hills, D.W. *J. Med. Chem.* **1967**, *10*, 1006.

(14) Sharpless, K. B.; Amberg, W.; Bennani, Y. L.; Crispino, G. A.; Hartung, J.; Jeong, K. S.; Kwong, H. L.; Morikawa, K.; Wang, Z. M.; Xu, D.; Zhang, X. L. *J. Org. Chem.* **1992**, *57*, 2768.

(15) Mangold, J. B.; Abdel-Monem, M. M. *J. Med. Chem.* **1983**, *26*, 66.

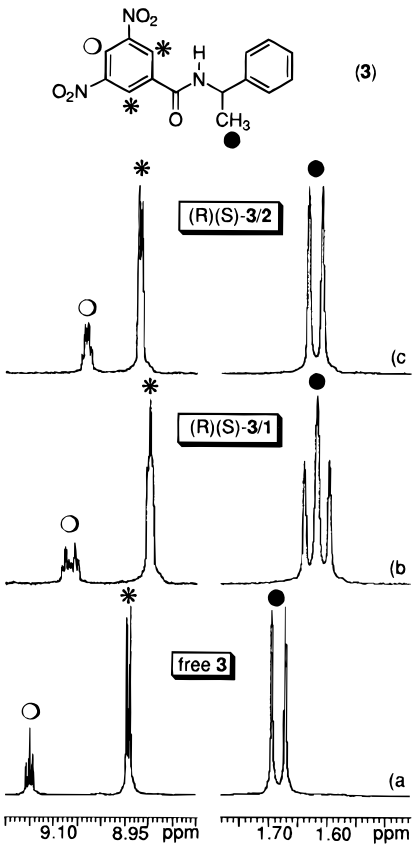

Figure 2. ^{1}H NMR (300 MHz, $CDCl_3$, ppm referenced to TMS as external standard, 25 °C) spectral regions corresponding to the 3,5-dinitrobenzoyl and methyl proton absorptions of (a) free compound **3** (28 mM), (b) equimolar mixture (*R*)(*S*)-**3**/**1**, and (c) equimolar mixture (*R*)(*S*)-**3**/**2**.

doubles significantly its 3,5-dinitrobenzoyl resonances (Figure 4a). Interestingly, the analogous compound **5b** is discriminated only by **2** (Figure 5), and both the complexation shifts and the nonequivalences are remarkably greater than those measured for **3** and **5a**. It is also to note that the interaction of each enantiomer of **5b** with **2** causes a relevant broadening of their proton absorptions, which could arise from a slowing down of their molecular motion due to the formation of transient diastereoisomeric species.

The enantiodiscriminating ability of **1** and **2** has been also probed in the case of 3,5-dinitrophenyl derivatives of amino acids (compound **6**), alcohols (compound **7**), and carboxyl acids (compound **8**). In these cases, smaller nonequivalences were measured ranging between 1.0 and 5.0 Hz for the 3,5-dinitrophenyl or alkyl protons.

Conformation and Dynamics of Benzoylated Cyclodextrins. As reported in the literature,[6,7] in DMSO solution, both cyclodextrins **1** and **2** show the pattern of ^{1}H NMR absorptions expected for a C_6 symmetry system: only one set of resonances is observed for each glucopyranosyl or aromatic proton.

On the contrary, a dramatic variation in the spectral parameters of **1** was observed in $CDCl_3$: two sets of signals, in an intensity ratio 1:1, for each proton or group of equivalent protons of the cyclodextrin are detected (Figure 6a). Only negligible chemical shift variations are found for **2** in the same solvent (Figure 6b).

Cyclodextrin 1. The doubling of the absorptions of **1**, observed in $CDCl_3$, reveals the presence of two different kinds of glucopyranoside units named A and B (Scheme 2).

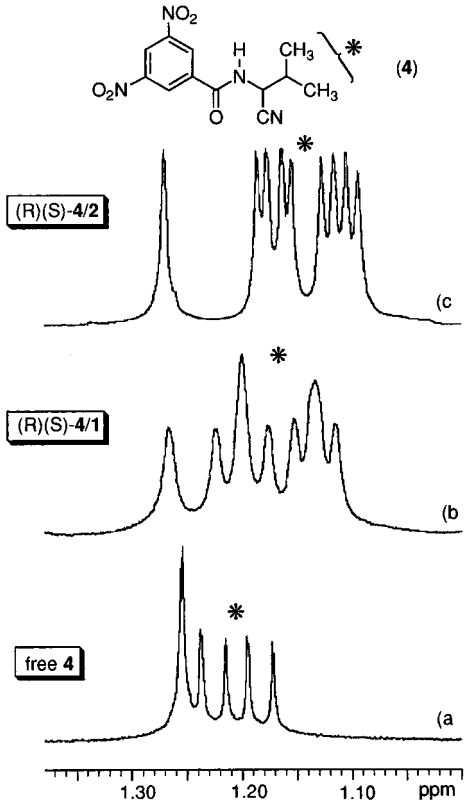

Figure 3. ^{1}H NMR (300 MHz, $CDCl_3$, ppm referenced to TMS as external standard, 25 °C) spectral regions corresponding to the methyl proton absorptions of (a) free compound **4** (36 mM), (b) equimolar mixture (*R*)(*S*)-**4**/**1**, and (c) equimolar mixture (*R*)(*S*)-**4**/**2**.

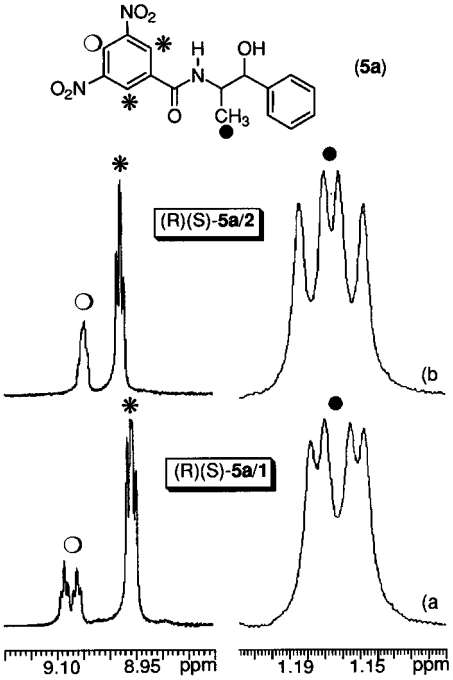

Figure 4. ^{1}H NMR (300 MHz, $CDCl_3$, ppm referenced to TMS as external standard, 25 °C) spectral regions corresponding to the 3,5-dinitrobenzoyl and methyl proton absorptions of **5a** (36 mM) of (a) equimolar mixture (*R*)(*S*)-**5a**/**1** and (b) equimolar mixture (*R*)(*S*)-**5a**/**2**.

The complete assignment of the proton absorptions (Table 1) required the combined use of 2D DQF-COSY and 2D ROESY analyses. The protons of each glucopyranoside unit, indicated as H_1-H_6 for A and $H_{1'}-H_{6'}$ for

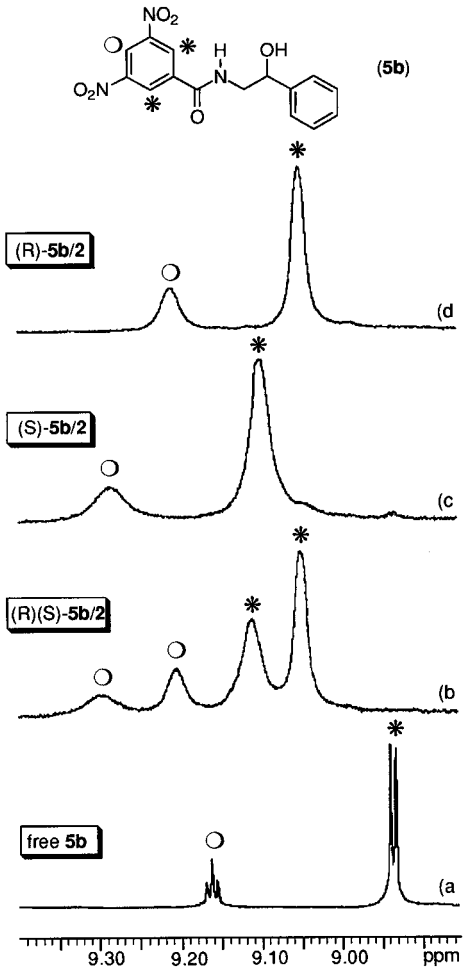

Figure 5. ^{1}H NMR (300 MHz, $CDCl_3$, ppm referenced to TMS as external standard, 25 °C) spectral regions corresponding to the 3,5-dinitrobenzoyl proton absorptions of (a) free compound **5b** (36 mM), (b) equimolar mixture (*R*)(*S*)-**5b**/**2**, (c) equimolar mixture (*S*)-**5b**/**2**, and (d) equimolar mixture (*R*)-**5b**/**2**.

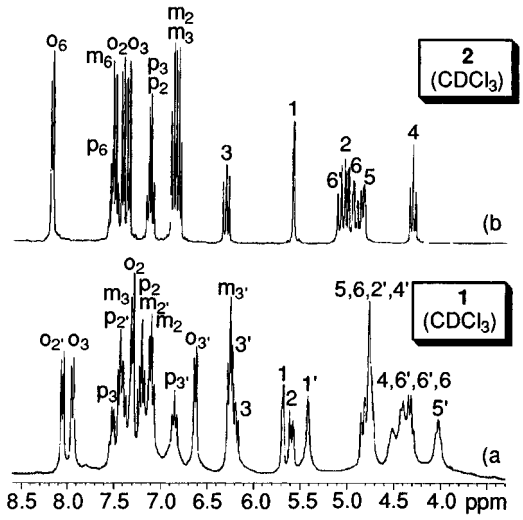

Figure 6. ^{1}H NMR (300 MHz, $CDCl_3$, 25 °C, 28 mM) spectrum of (a) **1** and (b) **2**.

B, have been simply assigned on the basis of the *J* correlations found in the COSY map. The precise assignment of each benzoyl group to the corresponding hydroxyl site required the analysis of the intraring NOEs measured in the 2D ROESY spectrum. In particular the doublet centered at 7.30 ppm has been assigned to the

Scheme 2

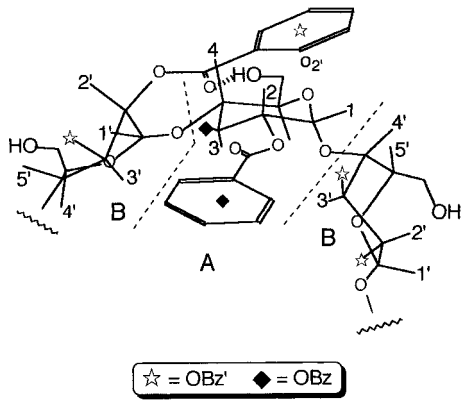

Table 1. ^{1}H NMR Chemical Shifts Data[a] (300 MHz, $CDCl_3$, 25 °C) of 1 and 2

	1		
	unit A	unit B[b]	2
H_1	5.68	5.42	5.67
H_2	5.59	4.82	5.00
H_3	6.18	6.25	6.29
H_4	4.31	4.75	4.29
H_5	4.70−4.90	4.02	4.83
H_6	4.30−4.60	4.30−4.60	4.89
H_6	4.70−4.90	4.30−4.60	5.08
H_o^2	7.30	8.07	7.39
H_m^2	7.09	7.20	6.86
H_p^2	7.29	7.40	7.11
H_o^3	7.95	6.61	7.34
H_m^3	7.43	6.24	6.81
H_p^3	7.52	6.84	7.13
H_o^6			8.17
H_m^6			7.49
H_p^6			7.52

[a] ppm referred to TMS as external standard. [b] Protons in the units B are indicated as $H_{1'}$, $H_{2'}$, etc.

ortho protons H_o^2 of the residue Bz^2 bound to the C_2-O site of A: they show an intense NOE on the proton H_1 at 5.68 ppm and a significant NOE on H_2 at 5.59 ppm (Figure 7, trace a). The ortho protons H_o^3 of Bz^3 of A were recognized as the ones giving the absorption at 7.95 ppm on the basis of the intense NOE produced on the H_3 proton (Figure 7, trace b). The proton absorptions of the two benzoyl groups $Bz^{2'}$ and $Bz^{3'}$ of the other glucopyranoside residue B have been assigned on the basis of the exchange effects observed in the 2D ROESY spectrum: the absorption at 8.07 ppm, showing the exchange peak (Figure 7, trace c) with the above ortho protons at 7.30 ppm (assigned to Bz^2), was attributed to the ortho protons $H_o^{2'}$ of $Bz^{2'}$. Analogously, the ortho protons at 6.61 ppm, originating the exchange peak with H_o^3 (Figure 7, trace d), were assigned to $H_o^{3'}$. The other aromatic protons were simply assigned on the basis of *J* correlations.

It is worth noting that the observability of the above exchange peaks in the 2D ROESY spectrum is also a clear indication that the two sets of protons, belonging to the glucopyranoside moieties A and B, are in slow interconversion on the NMR time scale.

The analysis of the 2D ROESY traces (Figure 7) also afforded clear indications on the relative stereochemistry of the two kinds of residues: the proton H_1 at 5.68 ppm of A (Figure 7, trace e) shows an intense NOE on the proton $H_{4'}$ (4.75 ppm) of the adjacent residue B, to indicate that these protons are cisoid. By contrast no inter-NOE $H_{1'}$−H_4 is observed. Accordingly, the ortho aromatic protons H_o^2 (Figure 7, trace a) originate NOEs

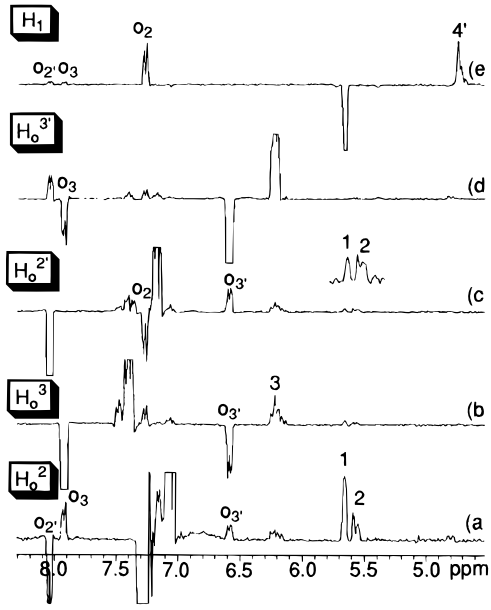

Figure 7. Traces of the 2D ROESY spectrum (300 MHz, $CDCl_3$, 25 °C, 28 mM, τ_m = 0.3 s) of **1** corresponding to (a) ortho protons H_o^2, (b) ortho protons H_o^3, (c) ortho protons $H_o^{2'}$, (d) ortho protons $H_o^{3'}$, and (e) H_1.

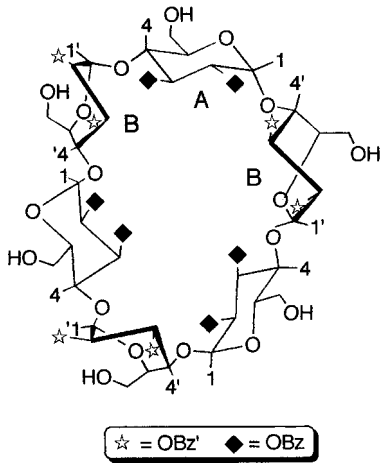

Figure 8. Conformational arrangement of **1** in $CDCl_3$ as derived by NMR data.

not only on the ortho aromatic protons H_o^3 belonging to the same residue A, but also on the ortho aromatic protons $H_o^{3'}$ of the adjacent residue B. The aromatic protons $H_o^{2'}$ (Figure 7, trace c) only produce NOE on the adjacent $H_o^{3'}$ protons of the same residue.

Therefore, by analyzing the triad BAB (Scheme 2), for the A unit, we find the proton H_1 faced to the proton $H_{4'}$ of the adjacent B unit and its proton H_4 far from the proton $H_{1'}$ of the unit B on the other side (Scheme 2). Analogously, for the unit B, the proton $H_{1'}$ is far from the proton H_4 of A and proton $H_{4'}$ cisoid to the proton H_1 of the residue A on the other side (Scheme 2).

Two different stereochemical pictures can be in keeping with the above discussed results: in a first structural arrangement three primary hydroxyl groups point toward the center of the cavity (as assessed by Lehn[6] and Stoddart,[7] Figure 1); in a second arrangement all the primary hydroxyl groups are disposed outside of the ring (Figure 8). However, the latter possibility has to be preferred on the basis of NOE data: inter-NOEs $H_o^{2'}$–H_2 and $H_o^{2'}$–H_1 between the ortho protons of $Bz^{2'}$ and the glucopyranoside protons H_1 and H_2 of the adjacent

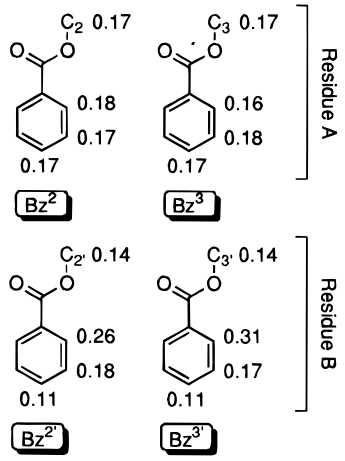

Figure 9. ^{13}C relaxation times (T_1, s) of the glucopyranoside and benzoyl carbons belonging to the two different residues A (Bz^2, Bz^3) and B ($Bz^{2'}$, $Bz^{3'}$) (A and B referenced to Scheme 2) of **1** in $CDCl_3$ (44 mM) solution.

unit are observed (Figure 7, trace c), whereas no inter-NOEs between the proton $H_{1'}$ and H_3 or Bz^3 are measured, as would expected when primary hydroxyl alternatively point toward the outside and inside of the ring (Figure 1).

Therefore, the introduction of benzoyl groups on the secondary hydroxyls of the cyclodextrin causes a severe distortion of the molecule, and the NOE data clearly show that all the primary hydroxyl groups of both units A and B point at the outside of the ring, as well as the two benzoyl groups $Bz^{2'}$ and $Bz^{3'}$ of B, whereas the two benzoyl groups Bz^2 and Bz^3 of the other residue A point toward the distorted cavity.

It is worthwhile to note that in such a stereochemical arrangement (Scheme 2) the $Bz^{2'}$ of B is in proximity of the primary hydroxyl group of the adjacent residue A, probably allowing a C=O···H–O hydrogen bond.

The $C_6 \rightarrow C_3$ reduction of the symmetry with respect to the unsubstituted cyclodextrin is also accompanied by a significant distorsion of the residue B, since its $H_{5'}$ proton does not originate any dipolar interaction with $H_{3'}$. Therefore, the residue B can be schematically represented as a twisted chair (Scheme 2) having the $H_{5'}$ and $H_{3'}$ protons far from each other and, hence, in a pseudoequatorial situation. Probably this distortion is the one required to have the alternating residues characterized by H_1 and $H_{4'}$ cisoid and $H_{1'}$ and H_4 far from each other.

The comparison between the longitudinal relaxation times of the methine carbons in the aromatic moieties with those of the glucosidic methines, to which they were bound, afforded valuable information on the relative rigidities of the aromatic nuclei of A and B (Figure 9).

All the aromatic methine carbons of the undistorted unit A (Figure 9) have relaxation times very similar (0.16–0.18 s) to that of the glucopyranoside carbons bearing the substituent. Therefore the aromatic rings of Bz^2 and Bz^3 follow the global motion of A, and they do not undergo independent motions about preferential axes. Rather different results were obtained for the B residue (Figure 9): the $C_{2'}$ and $C_{3'}$ methine T_1s (0.14 s) are shorter than those of ortho and meta methines of $Bz^{2'}$ and $Bz^{3'}$ (0.26 s for $C_{o2'}$, 0.18 s for $C_{m2'}$ and 0.31 s for $C_{o3'}$, 0.17 for $C_{m3'}$). Moreover these last T_1s are remarkably longer than those of the corresponding para methines (0.11 s). This is an indication that these aromatic residues undergo an anisotropic molecular motion around the long

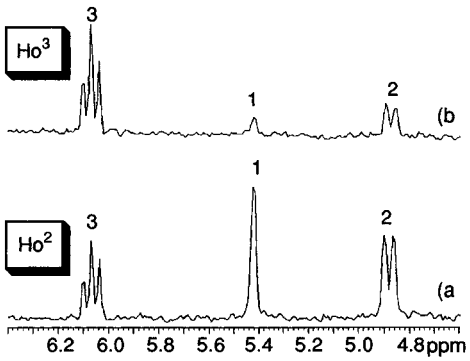

Figure 10. Traces of the 2D ROESY spectrum (300 MHz, DMSO, 25 °C, 28 mM, $\tau_m = 0.3$ s) of **1** corresponding to the ortho aromatic protons of the benzoyl group bound to (a) C_2-O site (H_o^2) and (b) C_3-O site (H_o^3).

molecular axis. The fast rotation around this axis contributes to the global relaxation of the ortho and meta carbons, and the effective rotational correlation time of *p*-C is longer than those of *m*-C or *o*-C.

These results are in keeping with our stereochemical model: the two benzoyls Bz^2 and Bz^3 of A are less free to rotate as they point toward the cavity, whereas the benzoyls $Bz^{2'}$ and $Bz^{3'}$ of B are more free to rotate as they point toward the outside.

The ^1H NMR spectrum of the same cyclodextrin, in DMSO as solvent, shows a signal pattern corresponding to a C_6 symmetry. Namely only one kind of glucopyranoside residue is present. The assignment of the benzoyls Bz^2 and Bz^3 bound to the ring carbons C_2-O and C_3-O, respectively, is immediately obtained by comparing in the 2D ROESY spectrum the traces of the two kinds of ortho protons resonating at 7.45 and 7.30 ppm (Figure 10, traces a, b): the first produce intense and comparable NOEs on H_3, H_2, and H_1 and the latter an intense NOE on H_3, but significantly minor NOEs on H_1 and H_2. Therefore, they must be assigned to the ortho protons of Bz^2 and Bz^3, respectively. Taking into account also that no NOE between H_o^2 or H_o^3 and H_4, directed toward the outside, is observed, we can conclude that both benzoyl groups are mainly bent toward the cavity.

Cyclodextrin 2. We have finally compared the conformational features in $CDCl_3$ of the cyclodextrin **1** with those of the cyclodextrin **2**, having spectral parameters in agreement with a C_6 symmetry. As above described, the benzoate units have been assigned to the corresponding sites on the glucopyranoside ring by an analysis in which 2D ROESY and 2D DQF-COSY data are compared. The most interesting traces of the 2D ROESY spectrum are collected in Figure 11. The protons at 8.17 ppm, originating NOEs on the protons H_6 and H_5, have been assigned to the ortho protons of Bz^6 (Figure 11, trace a). The absorption at 7.39 ppm has been attributed to the ortho protons of the benzoyl Bz^2 as they produce NOEs not only on the adjacent H_2 and H_3, but also an intense NOE on H_1 (Figure 11, trace b). Finally, the ortho protons at 7.34 ppm have been assigned to Bz^3 as they produce a more intense NOE on H_3 and a less intense NOE on H_2 (Figure 11, trace c).

The observability of inter-NOEs $H_o^6-H_5$ and $H_o^3-H_3$ or $H_o^2-H_3$ between ortho protons of the benzoate groups and internal protons of the cyclodextrin allow us to establish that these aromatic moieties are on the average faced to the two cavities of **2**, but their inclusion does not occur as no inter-NOEs between para aromatic protons and internal H_3 or H_5 are measured (Figure 12).

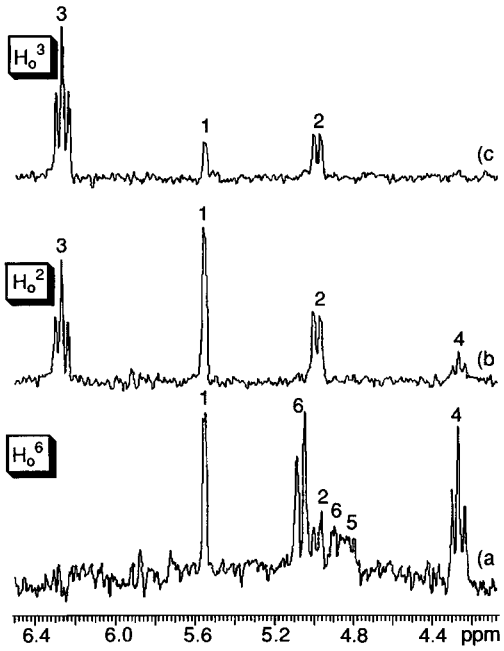

Figure 11. Traces of the 2D ROESY spectrum (300 MHz, $CDCl_3$, 25 °C, 28 mM, $\tau_m = 0.3$ s) of **2** corresponding to the ortho aromatic protons of the benzoyl group bound to (a) C_6-O site (H_o^6), (b) C_2-O site (H_o^2), and (c) C_3-O site (H_o^3).

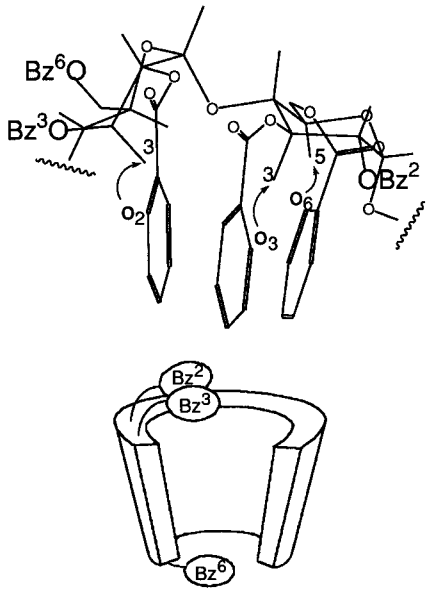

Figure 12. Conformational arrangement of **2** in $CDCl_3$ as derived by NMR data.

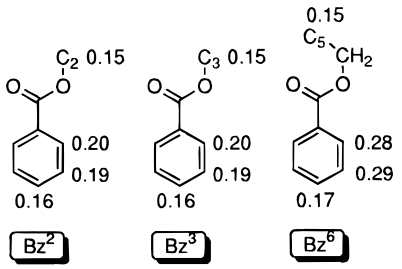

Figure 13. ^{13}C relaxation times (T_1, s) of the benzoate of **2** in $CDCl_3$ (74 mM) solution.

Once again, the carbon relaxation times (Figure 13) reflect the dynamic behavior of the cyclodextrin. These are rather homogeneous for the aromatic methine carbons of Bz^2 or Bz^3 and the methine directly linked to them

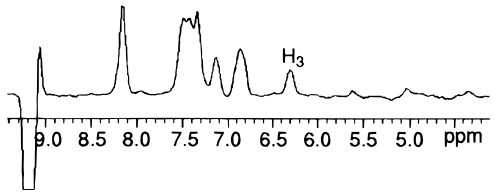

Figure 14. Trace of the 2D ROESY spectrum (300 MHz, $CDCl_3$, 25 °C, 80 mM, $\tau_m = 0.3$ s) of the mixture (*R*)-**5b**/**2** (molar ratio 1:1) corresponding to the para aromatic proton of the 3,5-dinitrobenzoyl moiety of **5b**.

(C_2 and C_3, respectively), whereas remarkably longer relaxation times are measured for the meta and ortho carbons of Bz^6 relatively to the para and C_5 carbons. This indicates that Bz^2 and Bz^3 are more rigid than Bz^6. Accordingly, the trace of the 2D ROESY map corresponding to the ortho protons $H_o{}^6$ of Bz^6 (Figure 11, trace a) shows an intense NOE with the external proton H_4, in addition to the above discussed NOE on the internal proton H_5.

Interaction Mechanism 2/(*R*)-5b and 2/(*S*)-5b. Attempts to obtain information on the interaction mechanism of **1** with the chiral substrates **3**−**8** by detection of the intermolecular dipolar interactions in the 2D ROESY maps of their mixtures failed probably as a consequence of the lability of the diastereoisomeric complexes formed. However, as evidenced above, the interaction of **2** with the two enantiomers of **5b** caused both a significant variation of the chemical shifts of (*S*)-**5b** or (*R*)-**5b** with respect to the free compounds and a remarkable broadening of their NMR absorptions (Figure 5). This clearly indicates that the diastereoisomeric complexes of (*S*)-**5b** and (*R*)-**5b** with **2** show higher stability constants than those of the complexes with **1** and also a high degree of conformational rigidity induced by the complexation. In fact, the analysis of the 2D ROESY spectra of the equimolar mixtures **2**/(*R*)-**5b** or **2**/(*S*)-**5b** allowed detection of inter-NOEs (Figure 14) between the 3,5-dinitrobenzoyl protons of (*R*)-**5b** or (*S*)-**5b** and the proton H_3 lying inside the cyclodextrin. No further intermolecular NOEs have been detected; therefore, the interaction between the enantiomers of **5b** and **2** takes place at the C_3 site of the cyclodextrin. This interaction seems to occur at the external surface of the cyclodextrin and probably no inclusion occurs taking into account that no inter-NOEs with the other internal proton H_5 are measured.

It is worthwhile to consider an interesting point arising from the comparison between the traces of the protons $H_o{}^3$ of the 2D ROESY maps of free **2** and its mixture with one or another enantiomer of **5b** (Figure 15), i.e. for free **2** the ortho protons of the benzoate (Bz^3) bound to C_3 does not produce NOE with H_4 (Figure 15, trace a); therefore, this benzoate must be faced to the wider cavity, as already discussed. By contrast, in the mixtures, the same proton (Figure 15, traces b, c) produces a relevant NOE on H_4 and, hence, it must be rotated toward the external part of the intermolecular complex.

Conclusions

The above described results allow the nature of the distortion introduced in α-cyclodextrin by benzoylation of the hydroxyl groups to be established. Compound **1** shows, in DMSO, a C_6 symmetry, and the benzoyl groups are faced to the wider cavity without undergoing inclusion. In $CDCl_3$, the symmetry of **1** reduces to C_3, and

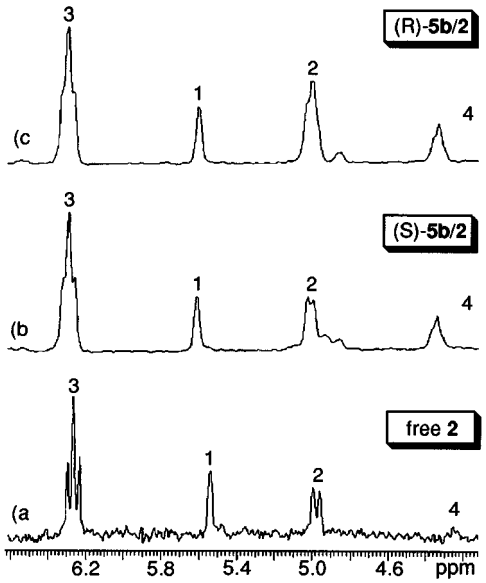

Figure 15. Ortho protons $H_o{}^3$ traces of the 2D ROESY spectra (300 MHz, $CDCl_3$, 25 °C, 80 mM, $\tau_m = 0.3$ s) of (a) free **2**, (b) equimolar mixture (*S*)-**5b**/**2**, and (c) equimolar mixture (*R*)-**5b**/**2**.

two different kinds of glucopyranoside residues are present: undistorted and distorted. The former maintains a chair-type conformation and the latter is a twisted-chair one. They reside alternatively on almost perpendicular planes and interchange. The benzoate groups at C_2 and C_3 of the undistorted residues point toward the cavity, whereas the same groups in the distorted residues point away from it (Figure 8). In this way all the primary hydroxyl groups are directed to the outside of the cyclodextrin; in particular, the hydroxyl function of the undistorted residue is close to the benzoate group at $C_{2'}$ site of the adjacent distorted residue, probably allowing the C=O···HO hydrogen bond formation.

Earlier investigations[6,7] on the same system led to a model where three hydroxyl groups point toward the center of the cavity creating a network of OH···OH hydrogen bonds (Figure 1). This structure is not in agreement with our NOE measurements. In this respect it is interesting to note that the same authors[7] report a C_6 symmetry for the analogous benzylated cyclodextrin ($PhCH_2$ *vs* PhCO) in which the benzyl groups could not hinder the formation of OH···OH hydrogen bonds. Therefore, the existence of interresidue C=O···H−O hydrogen bond seems better account for the $C_6 \rightarrow C_3$ transition.

As far as the perbenzoylated cyclodextrin **2** is concerned, the C_6 symmetry is retained and the exhaustive derivatization creates a closed structure where the benzoyl groups occlude both the wide and narrow rims and probably prevent the insertion of substrates. In spite of both the conformational distortion found for **1** and cavity crowding in **2**, the two cyclodextrins show enantiodiscriminating ability toward chiral substrates, and their use as chiral solvating agents for NMR spectroscopy can be proposed. However, since it seems unlikely that the enantiodiscrimination could originate from classical inclusion phenomena, superficial interactions of the chiral substrates with the polar functionalities of the derivatized cyclodextrin can be proposed. In the case of **2**, the noninclusive interaction with the enantiomers of **5b** has been proved to involve the C_3 site of the cyclodextrin and

to cause the rotation of the benzoyl groups toward the outside of the cavity.

Experimental Section

General Methods. NMR measurements were performed on a Varian VXR-300 spectrometer equipped with a temperature control unity (±0.1 °C). The 2D NMR spectra were obtained by using standard sequences. The double-quantum-filtered (DQF) COSY experiments were recorded with a spectral width of 1800 Hz; 512 increments of 8 scans and 2K data points were acquired. The relaxation delay was 5 s. The data were zero-filled to 2K × 1K, and a Gaussian function was applied for processing in both dimension. The HETCOR spectra were acquired with a spectral width of 11000 Hz in F_2 and 2000 Hz in F_1 in 2K data points using 32 scans of the 256 increments. The relaxation delay was 5 s. The data were zero-filled to 2K × 1K and a Gaussian function was applied for processing in both dimension. The phase-sensitive ROESY[10] spectra were acquired with a spectral width of 2000−3000 Hz in 2K data points using 8 scans for each of the 512 t_1 increments. The spin-lock time was set to 300 ms. The data were zero-filled to 2K × 1K, and a Gaussian function was applied for processing in both dimensions. The ^{13}C spin-lattice relaxation times were measured by the inversion-recovery method.

Thin layer chromatography (TLC) was carried out on silica gel plates (Merck, Silica G-60 0.2 mm), and compounds were visualized with iodine or by examination under UV light. Flash chromatography was carried out using Silica Gel 60 (Fluka, 0.035−0.070 mm particle size, 220−440 mesh ASTM).

High performance liquid chromatography (HPLC) was performed on a Perkin Elmer series 410 HPLC with UV detection at 254 nm, using a LiCrospher 100 RP-18 (5 μm) column. Solvent systems for chromatography are v/v.

Melting points were determined using a Koffler hot-stage apparatus. Optical rotations were measured using a Perkin Elmer 142 polarimeter.

Materials. Compound 1-cyano-1-amino-2-methylpropane was kindly provided by DMS Research (Geleen, The Netherlands). All chemicals were purified prior to use by standard methods.[16] α-Cyclodextrin was dried (12 h) at 110 °C/0.1 mmHg, in the presence of P_2O_5.

α-Cyclodextrin and 2-amino-1-phenyl-1-propanol hydrochloride were obtained from Fluka.

Hexakis(2,3,6-tri-*O*-benzoyl)-α-cyclodextrin (2). Following the experimental procedure reported,[6] chemically pure **2** (TLC benzene/ethanol = 4/1: R_f = 0.8; HPLC MeCN/H_2O = 85/15,1 mL/min: t_R = 30 min) having mp 157−160 °C, $[\alpha]^{22}_D$ +50.8 (*c* 1.04, $CHCl_3$) [lit.[6] $[\alpha]^{22}_D$ +54 (*c* 1, $CHCl_3$)], was recovered in 94% yield. ^1H NMR (DMSO-d_6, 25 °C, ppm referenced to TMS as external standard): 4.57 (H_4, 6H), 4.89 (H_5 and H_6, 12H), 5.10 (H_2, 6H), 5.14 (H_6, 6H), 5.65 (H_1, 6H), 6.25 (H_3, 6H), 6.87 ($H_m{}^3$, 12H), 6.98 ($H_m{}^2$, 12H), 7.24 ($H_p{}^3$, 6H), 7.27 ($H_p{}^2$, 6H), 7.28 ($H_o{}^3$, 12H), 7.49 ($H_o{}^2$, 12H), 7.52 ($H_m{}^6$, 12H), 7.61 ($H_p{}^6$, 6H), 8.13 ($H_o{}^6$, 12H). Anal. Calcd for $C_{162}H_{132}O_{48}$: C, 64.85%; H, 4.90%. Found: C, 64.81%; H, 4.93%.

Hexakis(2,3-di-*O*-benzoyl)-α-cyclodextrin (1). Compound **2** was converted into **1** according to Lehn.[6] Accurate purification of crude **1** by flash chromatography (benzene/ethanol = 6/1) gave (41% yield) a chemically pure sample (TLC benzene/ethanol = 6/1 R_f = 0.26; HPLC MeCN/H_2O = 85/15, 1 mL/min: t_R = 17.25 min) showing mp 207 °C (lit.[7] 209−210 °C), $[\alpha]^{22}_D$ +23.4 (*c* 1.14, $CHCl_3$) [lit.[6,7] $[\alpha]^{22}_D$ +9 (*c* 1.1, $CHCl_3$) and +11 (*c* 1, $CHCl_3$) respectively]. ^1H NMR (DMSO-d_6, 25 °C, ppm referenced to TMS as external standard): 3.88 (H_6, 6H), 4.17 (H_5, 6H), 4.26 (H_4, 6H), 4.40 (H_6, 6H), 4.89 (H_2, 6H), 4.93 (OH, 6H), 5.42 (H_1, 6H), 6.07 (H_3, 6H), 6.90 ($H_m{}^3$, 12H), 7.05 ($H_m{}^2$, 12H), 7.27 ($H_p{}^3$, 6H), 7.30 ($H_o{}^3$, 12H), 7.31 ($H_p{}^2$, 6H), 7.45 ($H_o{}^2$, 12H). Anal. Calcd for $C_{120}H_{108}O_{42}$: C, 68.34%; H, 4.68%. Found: C, 68.36%; H, 4.66%.

(*R*)- and (*S*)-2-Hydroxy-1-phenylethanol [(*R*)- and (*S*)-9]. According to the Sharpless recipe,[14] (*R*)-**9** and (*S*)-**9** were obtained starting from styrene (16.0 mmol) in quantitative yield after flash cromatography (ethyl acetate): mp 66 °C; $[\alpha]^{21}_D$ −38.1 (*c* 1.25, EtOH) for (*R*)-**9** and $[\alpha]^{21}_D$ +38.1 (*c* 1.25, EtOH) for (*S*)-**9** according to literature;[17] ^1H NMR ($CDCl_3$, 25 °C, ppm referenced to TMS as external standard): 2.30 (1H), 2.75 (1H), 3.60−3.80 (2H), 4.85 (1H), 7.20−7.50 (5H). Anal. Calcd for $C_8H_{10}O_2$: C, 69.54%; H, 7.30%. Found for (*R*)-**9**: C, 69.57%; H, 7.24%. Found for (*S*)-**9**: C, 69.52%; H, 7.23%.

(*R*)- and (*S*)-1-Phenyl-2-(tosyloxy)ethanol [(*R*)- and (*S*)-10]. A stirred solution of (*R*)-**9** (14.5 mmol) in 20 mL of anhydrous pyridine was treated, at −10 °C, with a stoichiometric amount of TsCl dissolved in the same solvent. The reaction mixture was stirred at −10 °C for 4 h and then quenched with ice−water. The organic materials were extracted with Et_2O, washed with HCl (10%), H_2O, $NaHCO_3$, and H_2O, and dried with Na_2SO_4. Ether was removed at reduced pressure to give 11.0 mmol (76% yield) of (*R*)-**10**: mp 65−66 °C, $[\alpha]^{21}_D$ −51.1 (*c* 1.00, $CHCl_3$). ^1H NMR ($CDCl_3$, 25 °C, ppm referenced to TMS as external standard): 2.10 (1H), 2.45 (3H), 4.00−4.20 (2H), 5.00 (1H), 7.30−7.40 (7H), 7.76−7.82 (2H). Anal. Calcd for $C_{15}H_{16}O_4S$: C, 61.63%; H, 5.52%; S, 10.95%. Found: C, 61.60%; H, 5.56%; S, 11.00%.

According to the above procedure, from (*S*)-**9** was obtained (*S*)-**10**: 78% yield, $[\alpha]^{21}_D$ +51.1 (*c* 1.00, $CHCl_3$). Anal. Calcd for $C_{15}H_{16}O_4S$: C, 61.63%; H, 5.52%; S, 10.95%. Found: C, 61.68%; H, 5.50%; S, 10.99%.

(*R*)- and (*S*)-2-Azido-1-phenylethanol [(*R*)- and (*S*)-11]. A solution of (*R*)-**10** (8.6 mmol) and NaN_3 (12.0 mmol) in DMF (70 mL) was stirred at 90−95 °C for 2 h. The reaction mixture was treated with H_2O, and the organic materials were extracted with Et_2O. After the usual workup, chromatographic elution (SiO_2, $CHCl_3$/petroleum ether 1:1 for the elution of byproducts, and $CHCl_3$/Et_2O 1:1 for the azido elution) yielded (93%) pure (*R*)-**11** as a colorless liquid: $[\alpha]^{19}_D$ −92.8 (*c* 1.08, $CHCl_3$). ^1H NMR ($CDCl_3$, 25 °C, ppm referenced to TMS as external standard): 2.45 (1H), 3.40−3.60 (2H), 4.85−4.95 (1H), 7.30−7.45 (5H). Anal. Calcd for $C_8H_9N_3O$: C, 58.87%; H, 5.56%; N, 25.76%. Found: C, 58.83%; H, 5.58%; N, 25.80%.

According to the above procedure, from (*S*)-**10** was obtained (*S*)-**11**: 90% yield, $[\alpha]^{19}_D$ +92.8 (*c* 1.08, $CHCl_3$). Anal. Calcd for $C_8H_9N_3O$: C, 58.87%; H, 5.56%; N, 25.76%. Found: C, 58.90%; H, 5.53%; N, 25.72%.

(*R*)- and (*S*)-2-Amino-1-phenylethanol [(*R*)- and (*S*)-12]. To a stirred suspension of $LiAlH_4$ (32.7 mmol) in dry Et_2O (100 mL) a solution of (*R*)-**11** (7.4 mmol) in the same solvent (50 mL) was added. The reaction mixture was refluxed for 3 h, stirred at room temperature for 12 h, hydrolyzed with ice−water, and filtered. After the usual workup, (*R*)-**12** was recovered (90% yield): mp 52−55 °C, $[\alpha]^{23}_D$ −45.0 (*c* 1.32, C_6H_6) according to the literature.[18] ^1H NMR ($CDCl_3$, 25 °C, ppm referenced to TMS as external standard): 1.90 (3H), 2.70−3.10 (2H), 4.60 (1H), 7.20−7.40 (5H). Anal. Calcd for $C_8H_{11}NO$: C, 70.04%; H, 8.08%; N, 10.21%. Found: C, 70.00%; H, 8.10%; N, 10.23%.

According to the above procedure, from (*S*)-**11** was obtained (*S*)-**12**: 80% yield; $[\alpha]^{23}_D$ +45.0 (*c* 1.32, C_6H_6) according to the literature.[18] Anal. Calcd for $C_8H_{11}NO$: C, 70.04%; H, 8.08%; N, 10.21%. Found: C, 70.03%; H, 8.03%; N, 10.22%.

3,5-Dinitrobenzoyl Derivatives of 5.[12] A tetrahydrofuran solution (300 mL) of 3,5-dinitrobenzoic acid (15.0 mmol) and 2-ethoxy-1-(ethoxycarbonyl)-1,2-dihydroquinoline (EEDQ) (15.0 mmol) was stirred for 3 h, and then the suitable β-hydroxyphenethylamine (15.0 mmol) was added. The reaction mixture was stirred at room temperature overnight, and then the solvent was removed at reduced pressure. The crude residue, crystallized from $CHCl_3$/pentane (1:3), gave pure **5a,b**.

2-(3′,5′-Dinitrobenzamido)-1-phenyl-1-propanol (**5a**): mp 129−131 °C. ^1H NMR ($CDCl_3$, 25 °C, ppm referenced to TMS as external standard): 1.14 (3H), 2.55 (1H), 4.53 (1H), 5.02 (1H), 6.57 (1H), 7.26−7.50 (5H); 8.91 (2H), 9.14 (1H). Anal.

(16) Perrin, D. D.; Armarego, W. L. F.; Perrin, D. R. *Purification of laboratory chemicals*; Pergamon Press: Toronto, 1983.

(17) King, R. B.; Bakos, J.; Hoff, C. D.; Markó, L. *J. Org. Chem.* **1979**, *44*, 1729.

(18) Ziegler, T.; Hörsch, B.; Effenberger, F. *Synthesis* **1990**, 575.

Calcd for $C_{16}H_{15}N_3O_6$: C, 55.65%; H, 4.38%; N, 12.17%. Found: C, 55.61%; H, 4.40%; N, 12.20%.

(*R*)- and (*S*)-2-(3′,5′-Dinitrobenzamido)-1-phenylethanol [(*R*)- and (*S*)-**5b**]: mp 95 °C. ^{1}H NMR ($CDCl_3$, 25 °C, ppm referenced to TMS as external standard): 2.92 (1H), 3.56 (1H), 4.01 (1H), 5.00 (1H), 6.88 (1H), 7.30−7.50 (5H), 8.94 (2H), 9.16 (1H). Anal. Calcd for $C_{15}H_{13}N_3O_6$: C, 54.38%; H, 3.96%; N, 12.69%. Found for (*R*)-**5b**: C, 54.41%; H, 3.94%; N, 12.66%. Found for (*S*)-**5b**: C, 54.36%; H, 3.98%; N, 12.71%.

Characterization Data of 3, 4, 6, 7, and 8. 1-Phenyl-1-(3′,5′-dinitrobenzamido)ethane (**3**): mp 145 °C. ^{1}H NMR ($CDCl_3$, 25 °C, ppm referenced to TMS as external standard): 1.68 (3H), 5.36 (1H), 6.81 (1H), 7.27−7.50 (5H), 8.94 (2H), 9.15 (1H). Anal. Calcd for $C_{15}H_{13}N_3O_5$: C, 57.14%; H, 4.16%; N, 13.33%. Found: C, 57.10%; H, 4.18%; N, 13.30%.

1-Cyano-1-(3′,5′-dinitrobenzamido)-2-methylpropane (**4**): mp 127−129 °C. ^{1}H NMR ($CDCl_3$, 25 °C, ppm referenced to TMS as external standard): 1.18 (3H), 1.22 (3H), 2.25 (1H), 5.04 (1H), 6.84 (1H), 8.99 (2H), 9.23 (1H). Anal. Calcd for $C_{12}H_{12}N_4O_5$: C, 49.31%; H, 4.14%; N, 19.17%. Found: C, 49.34%; H, 4.11%; N, 19.20%.

N-(3,5-dinitrobenzoyl)alanine methyl ester (**6**):[8] ^{1}H NMR ($CDCl_3$, 25 °C, ppm referenced to TMS as external standard): 1.60 (3H), 3.85 (3H), 4.85 (1H), 7.55 (1H), 8.90 (2H), 9.15 (1H).

t-2-Ethoxy-*r*-1-(hydroxymethyl)-1-methylcyclobutane 3,5-dinitrobenzoate (**7**):[9] ^{1}H NMR ($CDCl_3$, 25 °C, ppm referenced to TMS as external standard): 1.21 (3H), 1.26 (3H), 1.57 (2H), 2.02 (1H), 2.22 (1H), 3.43 (1H), 3.48 (1H), 3.84 (1H), 4.29 (1H), 4.36 (1H), 9.15 (2H), 9.23 (1H).

N-(3′,5′-Dinitrophenyl)-2-(*p*-isobutylphenyl)propionamide (**8**): mp 195−200 °C. ^{1}H NMR ($CDCl_3$, 25 °C, ppm referenced to TMS as external standard): 0.95 (6H), 1.63 (3H), 1.85 (1H), 2.49 (2H), 3.80 (1H), 7.23 (4H), 7.71 (1H), 8.72 (3H). Anal. Calcd for $C_{19}H_{21}N_3O_5$: C, 61.45%; H, 5.70%; N, 11.31%. Found: C, 61.41%; H, 5.66%; N, 11.35%.

Acknowledgment. This work has been partially supported by CNR, Roma, Italy.

Supporting Information Available: ^{1}H NMR spectra of **1** and **2** in DMSO-d_6 at 25 °C; 2D DQF-COSY and 2D ROESY maps of **1** in $CDCl_3$; scheme summarizing the characterization strategy for **1** (4 pages). This material is contained in libraries on microfiche, immediately follows this article in the microfilm version of the journal, and can be ordered from the ACS; see any current masthead page for ordering information.

JO961562X